$LaPO_4$:Ce,Tb and YVO_4:Eu nanophosphors: Luminescence studies in the vacuum ultraviolet spectral range

V. Pankratov,[1,a] A. I. Popov,[1,2] L. Shirmane,[1] A. Kotlov,[3] and C. Feldmann[4]
[1]*Institute of Solid State Physics, University of Latvia, 8 Kengaraga, Riga LV-1063, Latvia*
[2]*Institute Laue Langevin, 6 rue Jule Horovitz, Grenoble 38042, France*
[3]*HASYLAB at DESY, Notkestrasse 85, Hamburg D-22607, Germany*
[4]*Institute of Inorganic Chemistry, Karlsruhe Institute of Technology (KIT), Engesserstrasse 15, Karlsruhe D-76131, Germany*

(Received 16 June 2011; accepted 5 August 2011; published online 14 September 2011)

Comparative analysis of the luminescent properties of nanocrystalline $LaPO_4$:Ce,Tb and YVO_4:Eu luminescent materials with macrocrystalline analogues, commercially produced by Philips, has been performed under excitation by pulsed vacuum ultraviolet (VUV) synchrotron radiation, ranging from 3.7-40 eV. Special attention was paid to VUV spectral range, which is not reachable with commonly used lamp and laser sources. Our results clearly show distinct difference in the excitation spectra for nano- and macrocrystalline samples, especially at energies, when the spatial separation of electron-hole pairs is comparable with sizes of nanoparticles. Differences in the region of multiplication of the electronic excitations are also demonstrated and discussed. © *2011 American Institute of Physics*. [doi:10.1063/1.3634112]

I. INTRODUCTION

Oxide luminescent materials $LaPO_4$ and YVO_4 doped with lanthanide ions have been extensively studied as prospective materials in the fields of high-resolution optical devices, such as color television cathode ray tubes, high-pressure mercury lamps, electroluminescent and field emission displays, or as nanophosphors for biological labeling and bifunctional magnetic-luminescent nanocomposites.[1–16] These phosphors are characterized by their high energy-conversion efficiency, purity in spectral colors, and high thermal stability. They have the advantage over the currently used sulfide phosphors in stability in vacuum and absence of corrosive gas emission under electron bombardment.[17]

One of the materials discussed in this paper is YVO_4:Eu. Since Levine and Palilla[1] in 1964 developed the Eu^{3+}-doped YVO_4 as a red phosphor for the commercial applications in color television cathode ray tube displays and high-pressure mercury lamps, there has been extensive study on this material doped with different lanthanide ions, such as Er^{3+}, Sm^{3+}, and Dy^{3+}. Luminescence properties of YVO_4:Eu^{3+} crystals and related materials have been studied for more than three decades.[1–3,6,7,15,18–21] The absorption spectrum of YVO_4 shows strong and broad bands in the ultraviolet (UV) region. The absorption transition involved is a charge transfer from oxygen 2p to the vanadium 3d states, forming excited $(VO_4)^{3-}$ molecular complex. Considerably small Stokes shift of the emission from such $(VO_4)^{3-}$ vanadate group leads to favorable conditions for thermally activated energy migration. Thus, bulk YVO_4:Eu^{3+} shows strong red emission under UV illumination due to efficient energy transfer from excited $(VO_4)^{3-}$ complex anions to Eu^{3+} activator ions. Quantum yields as high as 70% are reported, providing the bulk YVO_4:Eu^{3+} material as one of the most important phosphor compounds.

In 1998, Hasse and Riwotzki first applied the hydrothermal method in the synthesis of lanthanide-doped YVO_4 nanocrystalline powers, which were weakly dispersed as an aqueous colloid.[3] In 2000, Huignard *et al.*[6] gained the concentrated colloidal solutions of well-dispersed YVO_4:Eu^{3+} nanoparticles by precipitation reactions at room temperature. Later, they synthesized colloidal YVO_4:Eu^{3+} nanoparticles with a diameter of $\sim$8 nm,[7] and in the colloids, the YVO_4:Eu^{3+} nanoparticles also have a relatively high quantum efficiency and brightness in comparison with the other rare-earth doped nanophosphors.[3,6,7] Consequently, the luminescence properties of YVO_4:Eu^{3+} nanoparticles have aroused great interest. Among the different host materials researched, much attention has been given especially to YVO_4:Eu^{3+} also, because it can be crystallized at low temperatures to obtain much smaller nanocrystals more easily. Nevertheless, YVO_4:Eu nanoparticles have still comparably low (about 20%) quantum yield,[3,4,21] which is much lower than the quantum yield for bulk YVO_4:Eu. One of the possible reasons of low luminescence efficiency in YVO_4:Eu nanoparticles could be surface loss processes. In order to suppress them, it was suggested to apply core shell layers of YF_3 around YVO_4:Eu nanoparticles.[22] Comparison of luminescence properties for bulk, nano, and core-shelled nano YVO_4:Eu will be extremely useful for the understanding of surface loss processes, as well as it could help modify nanosized YVO_4:Eu in order to get nanopowders with high quantum yield.

Another material discussed in this paper, lanthanum phosphate ($LaPO_4$), also known as monazite, has been widely used as a phosphor and proton conductor, as well as in sensors, lasers, ceramic materials, catalysts, and heat-resistant

[a]Author to whom correspondence should be addressed. Electronic mail: vpank@latnet.lv. Fax: +371-67 132 778.

materials. This is due to its interesting properties, such as very low solubility in water, high thermal stability, high index of refraction, and so on.[23–27] Rare earth orthophosphates as host matrices—and $LaPO_4$ in particular—also exhibit quite a good ionizing and particle radiation as well as photochemical stability. This is why $LaPO_4$ has been also suggested as a prospective waste form for high-level nuclear waste.[28,29]

In recent years, $LaPO_4$ has been also shown to be a useful host lattice for lanthanide ions to produce phosphors that emit in a broad range of colors.[23,27,30–32] Even in 1963, it was already known that $LaPO_4$:0.01Ce^{3+} is a "short luminescence delay time phosphor" and emits ultraviolet (UV) light, which peaks spectrally at about 340 nm, when excited with cathode rays, and its luminescence decay time is about 24 ns.[33] Doping with different types of rare earth ions (Eu^{3+}, Ce^{3+}, Tb^{3+}, Nd^{3+}, Er^{3+}, Pr^{3+}, Ho^{3+}, Yb^{3+}, Tm^{3+}) in macro- as well as nanosized $LaPO_4$ has been frequently reported in the literature. Among all these phosphate-type phosphors, trivalent cerium (Ce^{3+}) and terbium (Tb^{3+}) co-activated $LaPO_4$ ($LaPO_4$:Ce,Tb) bulk powder is known as most efficient because of the high-efficiency energy transfer between Ce^{3+} and Tb^{3+}.[23,27,30–32] Bulk $LaPO_4$:Ce,Tb is also intensely used as an excellent green emitting phosphor for fluorescent lamps.[27,34,35] Nowadays, $LaPO_4$:Ce,Tb is known as one of the most promising highly luminescent green phosphors which is one of the best candidates for biomedical applications, such as fluorescence resonance energy transfer (FRET) assays, biolabeling, optical imaging, or phototherapy,[36–38] where green emission from Tb^{3+} is highly important. However, under UV excitation (for instance, under 254-nm radiation of mercury discharge lamps), only forbidden f-f transitions of Tb^{3+} in $LaPO_4$ could be excited and, therefore in this case, Tb^{3+} emission is not efficient. On the other hand, allowed f-d transition in a Tb^{3+} ion lays at much higher energies, i.e., at VUV spectral range. Thus, in order to effectively absorb relatively low energy UV light, a sensitizer should be used. In $LaPO_4$ phosphor, Ce^{3+} ions with effective 4f-5d absorption behave as the sensitizer, whereas Tb^{3+} ions act as the luminescent center. Indeed, under UV excitation of Ce^{3+} ion, a $4f^1 \rightarrow 4f^05d^1$ transition occurs. After energy transfer from Ce^{3+} to Tb^{3+}, a green Tb^{3+} emission resulting from $^5D_4 \rightarrow {}^7F_J$ relaxation takes place. Despite luminescence properties of bulk $LaPO_4$:Ce,Tb, as well as energy transfer processes between Ce^{3+} and Tb^{3+} ions, which have been intensively studied before,[34,39–42] we have recently suggested alternative mechanism of energy transfer via the so-called impurity trapped exciton states in nanosized $LaPO_4$:Ce,Tb[43] by analogy with some other wide bandgap materials.[44–46]

Most of the studies reported in the literature were performed using laser or ultraviolet lamps as an excitation sources, while, for instance, $LaPO_4$ belongs to the class of wideband-gap materials, and its experimental bandgap was reported to be around 8.0 eV.[47,48] To extend the excitation energy range, in this paper, we use the pulsed synchrotron radiation, which, due to its broad and continuous spectrum, is a very useful tool for the investigation of optical and luminescence properties of wideband-gap materials,[49–54] where UV and VUV excitations are dominant.

II. EXPERIMENT

A. Nanophosphors synthesis

Both types of luminescent $LaPO_4$:Ce,Tb and YVO_4:Eu nanopowders were produced via a microwave-accelerated synthesis in ionic liquids. This method was described in detail elsewhere.[22,55–57]

The crystallinity of as prepared $LaPO_4$:Ce,Tb is proven by powder x ray diffraction (PXRD) pattern[55] as well as by high-resolution transmission electron microscopy (HRTEM). Both types of method—as expected—indicate the nanoparticles to crystallize with the monazite type of structure. With the assumption of spherical particles, a mean particle diameter of 8–10 nm is calculated using Scherrer's equation. This value agrees with that determined by electron microscopy.[55] The dopant concentration of 45 mol. % Ce^{3+} and 15 mol. % Tb^{3+} is quite common for $LaPO_4$:Ce,Tb phosphors.[34] Due to the similar radii of the three-valent rare-earth ions, phase separation does not occur.[34,35] The composition and the amount of dopants are confirmed by energy-dispersive x ray analysis (EDX). Pressed pellets of the as-prepared nanopowder show values of: 39 (1) mol. % La (expected 40 mol. %), 46 (1) mol. % Ce (expected 45 mol. %), and 15 (1) mol. % Tb (expected 15 mol. %). Commercial macroscopic $LaPO_4$:Ce,Tb powder with the same dopants level was also used in the current study as a reference material in the luminescence measurements.

The details of the synthesis procedure of YVO_4:Eu nanopowders, as well as the result of the sample's characterizations by means of electron microscopy, energy loss spectroscopy, infrared spectroscopy, dynamic light scattering (DLS), and x ray diffraction analysis (XRD), have been reported in Ref. 22. According to electron microscopy, DLS, and XRD, the presence of uniform and highly crystalline particles, 12–15 in diameter, is validated. As-prepared particles turn out to be non-agglomerated and redispersible. Commercial bulk YVO_4:Eu powder (with particle size several microns) from Phillips was also characterized by means of UV-VUV luminescence spectroscopy for comparison. The dopant level in nanosized YVO_4:Eu was 15 mol. %, whereas bulk YVO_4:Eu was typically doped with 5 mol. %. In order to minimize possible surface-related losses, YVO_4:Eu nanoparticles have been covered by a nonluminescent 1-2 nm thickness YF_3 layer, as was described in Ref. 22. Such a sample is denoted in the paper as YVO_4:Eu@YF_3.

B. Luminescence characterization

In the present study, luminescence properties of nanophosphors in the UV-VUV spectral range were studied with pulsed synchrotron radiation from the DORIS III storage ring of the Deutsches Elektronen-Synchrotron DESY (Hamburg, Germany). The Superlumi experimental station of HASYLAB was used for the measurements of emission and excitation spectra.[58] The excitation spectra were recorded in the 330-30 nm (3.7-40 eV) spectral range with a spectral resolution of 0.3 nm. Excitation spectra of sodium salicylate were normalized to equal synchrotron radiation intensities impinging onto the sample. Luminescence spectra in the UV

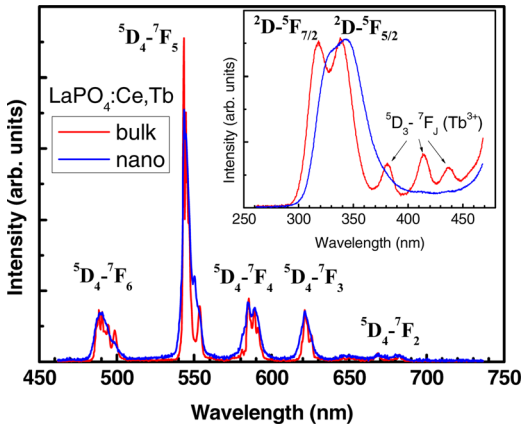

FIG. 1. (Color online) Emission spectra of Tb^{3+} and Ce^{3+} ions (inset) in the macroscopic and nanosized $LaPO_4$:Ce,Tb under excitation in the Ce^{3+} absorption band (250 nm) at 10 K.

and visible/infrared range were recorded with a monochromator (SpectraPro-308i, Acton Research Corporation) equipped with a liquid nitrogen-cooled CCD detector (Princeton Instruments) and a photomultiplier (HAMAMATSU R6358P). The spectral resolution of the analyzing monochromator was typically 11 nm. Emission spectra were corrected for the spectral response of the detection system. Powders were slightly pressed into pellets and installed onto the sample holder of a flow-type liquid helium cryostat.

It is necessary to note that both materials belong to the class of radiation-resistant oxide materials in which radiation damage occurs via particles elastic collisions only; that is not the case for 3.7-40 eV photons.[59,60]

III. RESULTS AND DISCUSSION

A. $LaPO_4$:Ce,Tb

Let us start with demonstration of distinctions in luminescence properties (especially in the VUV range) between bulk and nanosized $LaPO_4$:Ce,Tb. Emission spectra of Tb^{3+} and Ce^{3+} ions for both bulk and nanosized $LaPO_4$:Ce,Tb are demonstrated in Fig. 1. The spectra were excited by 250-nm photons, which correspond to a $4f^1 \rightarrow 4f^05d^1$ transition in the Ce^{3+} ion. From Fig. 1, it is clearly seen that a significant discrepancy between emission spectra for bulk and nano samples takes place. Detailed analysis of the emission spectra was done in Ref. 54, taking into account fine structures of both Ce^{3+} and Tb^{3+} emission bands. It was suggested there that a strong perturbation of the crystal field of rare-earth ions due to a small nanoparticle size leads to the changes in the emission spectra.

The excitation spectra for both Ce^{3+} and Tb^{3+} emissions are depicted in Figs. 2(a) and 2(b) for the bulk and the nanosized $LaPO_4$:Ce,Tb samples, respectively. The excitation spectrum of Ce^{3+} emission in the 4.0–6.5 eV range for the bulk $LaPO_4$:Ce,Tb (Fig. 2(a)) ordinates due to 4f-5d transition in Ce^{3+} ion in $LaPO_4$ matrix. This spectrum is composed of five bands peaking at 4.46 eV, 4.76 eV, 5.2 eV, 5.8 eV, and 6.05 eV, which are due to the transition from the ground state $^2F_{5/2}$ ($4f^1$) to the five crystal-field split levels of the ^2D ($5d^1$) excited state in the $LaPO_4$ lattice. These bands are similar to those observed for cerium-doped $LaPO_4$ and reported before in Ref. 61.

The low energy part of the excitation spectrum of Tb^{3+} emission, where f-f transition in Tb^{3+} occur (4.0–5.6 eV), is very close to the excitation spectrum of Ce^{3+} emission (Fig. 2(a)). Note, according to Ref. 61, such intensive excitation is practically negligible in the excitation spectrum of Tb^{3+} emission in terbium-doped $LaPO_4$. Taking into account that f-f transitions of Tb^{3+} emission are not effective in this spectral range, it is naturally concluded that the intensive excitation of Tb^{3+} emission in the 4.0–5.6 eV range appears due to energy transfer from Ce^{3+} to Tb^{3+}. On the other hand, f-d transitions in Tb^{3+} ions become dominant at energies higher than 5.6 eV and, therefore, Tb^{3+} emission can be excited directly, i.e., without energy transfer via Ce^{3+} states. A crystal-field splitting is responsible for a prodigious structure of the Tb^{3+} excitation spectrum at energies higher than 5.6 eV (Fig. 2(a)). In this case, the transitions from the ground state ^7F ($4f^8$) to the lowest ^7D ($4f^75d$) and to the lowest ^9D ($4f^75d$) term leads to formation of ten bands in the Tb^{3+} excitation spectrum (Fig. 2(a)) in the 5.6–7.7 eV range. These bands are described in detail in Ref. 12 for terbium-doped bulk $LaPO_4$.

The excitation spectrum for Ce^{3+} emission in nanosized $LaPO_4$:Ce,Tb has intensive bands in the 3.5–6.5 eV spectral range (Fig. 2(b)), which are qualitatively similar to the corresponding excitation obtained for bulk $LaPO_4$:Ce,Tb in Fig.

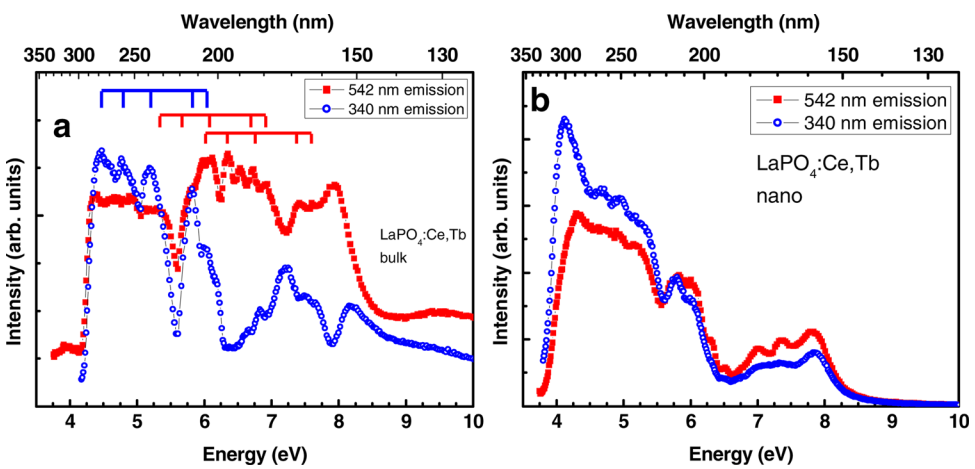

FIG. 2. (Color online) Excitation spectra of Ce^{3+} (340 nm) and Tb^{3+} (542 nm) emissions in the macroscopic (a) and nanosized (b) $LaPO_4$:Ce,Tb at 10 K. The positions of crystal-field split Ce^{3+} and Tb^{3+} bands in $LaPO_4$:Ce and $LaPO_4$:Tb obtained in Ref. 61 are demonstrated by red and blue scale lines for comparison.

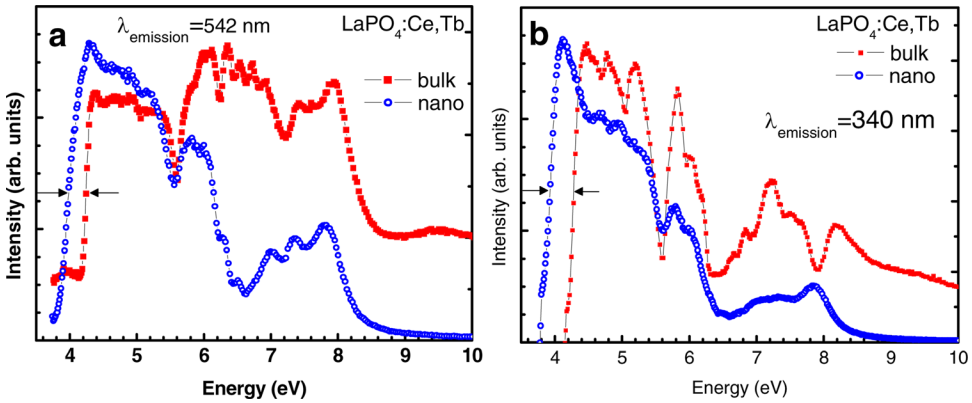

FIG. 3. (Color online) Comparison of excitation spectra of Tb^{3+} (542 nm) (a) and Ce^{3+} (340 nm) (b) emissions for bulk and nanosized $LaPO_4$:Ce,Tb at 10 K in 3.5–10 eV spectral range.

2(a). On the other hand, the excitation spectrum of Tb^{3+} emission in the nano sample is drastically changed compared with the bulk one. Indeed, the part of the excitation spectrum due to f-d transitions in the Tb^{3+} ion (5.6 eV and higher) is significantly suppressed in nano $LaPO_4$:Ce,Tb. This result is in contradiction to the Tb^{3+} excitation spectrum in the bulk sample, where significant contribution of f-d transition in Tb^{3+} was detected in the 5.6–7.7 eV range (Fig. 2(a)). It means that Tb^{3+} ions practically cannot be directly excited in nanosized $LaPO_4$:Ce,Tb, but could be excited after energy transfer from Ce^{3+} only. We suggest that, due to small nanoparticle size and high impurity concentration, Tb^{3+} and Ce^{3+} ions are closely distributed, i.e., no isolated Tb^{3+} ions in nanoparticles. Since a cerium concentration is three times higher than a terbium one, Ce^{3+} ions "shield" Tb^{3+} ions, and Ce^{3+} ions' excitation is very probable.

In fact, the distinctions in the excitation spectra between bulk and nano samples for both Ce^{3+} and Tb^{3+} emissions are especially well demonstrated in Fig. 3 and Fig. 4. First of all, it is evident that, exploring the low energy part of the excitation spectra, a redshift is detected in the excitation spectra for the nano sample (pointed by arrows on Fig. 3). This redshift looks the same for both Ce^{3+} and Tb^{3+} emissions. As we already mentioned above, Tb^{3+} emissions are excited via Ce^{3+} states at energies below 5.6 eV. Therefore, it is natural that the excitation spectrum of Tb^{3+} has similar peculiarities comparing with the excitation spectrum of Ce^{3+} emission in this spectral range. It is supposed that the redshift of the excitation spectra is due to perturbation of 5d levels of Ce^{3+} ions in nanosized $LaPO_4$:Ce,Tb. As a result of such perturbation, the 5d excited state is slightly shifted and Ce^{3+} excitation spectrum in nano $LaPO_4$:Ce,Tb is shifted to the low energy side, comparing with the corresponding spectrum for the bulk sample.

Other significant differences between the excitation spectra for bulk and nano $LaPO_4$ (Fig. 3) are clearly revealed in the 6.5-8.5 eV spectral range. Taking into account bandgap energy of $LaPO_4$ (8 eV), the excitation bands in this spectral range could belong to excitonic excitation bands (including self-trapped and/or bound excitons). Optical properties of excitons are extremely sensitive to nanoparticle size, due to the increasing role of surface effects. Thus, the changes in the excitation spectra in the 6.5-8.5 eV spectral range could be induced by the nanoparticle's surface on the excitons in nanosized $LaPO_4$. For instance, the excitation bands of the bound exciton near Ce^{3+} are well resolved in the 6.5-8.0 eV range in bulk $LaPO_4$:Ce,Tb, whereas these bands are significantly smoothed and suppressed in the nanopowder (Fig. 3(b)), obviously due to surface influence.

Important information could be retrieved from Fig. 4 examining the excitation spectra at energies higher than 8 eV. In contrast to the bulk material, both Ce^{3+} and Tb^{3+} emissions practically could not be excited in the nanopowders if the excitation energy exceeds the bandgap energy of

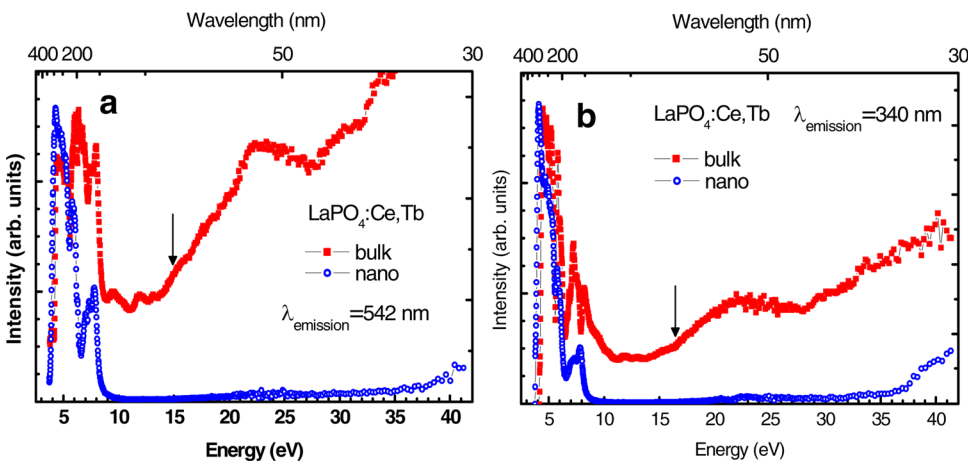

FIG. 4. (Color online) Comparison of excitation spectra of Tb^{3+} (542 nm) (a) and Ce^{3+} (340 nm) (b) emissions for bulk and nanosized $LaPO_4$:Ce,Tb at 10 K in wide spectral range (3.5–40 eV). Black arrows point out the initial stage of MEE processes.

$LaPO_4$. This fact clearly indicates that there is no energy transfer from the $LaPO_4$ matrix to the Ce^{3+} and Tb^{3+} ions in nanoparticles. Processes occurring under high energy excitations could be briefly considered as follows: After high energy excitations (higher than 8 eV), electrons in the conduction band and holes in the valence band are created. In the bulk sample, after some relaxations, electrons and holes are trapped by dopants, forming excited Ce^{3+} and Tb^{3+} ions, and their radiative relaxation leads to Ce^{3+} and Tb^{3+} emissions. On the other hand, electrons and holes in the nanoparticles could be easily trapped by surface defects, where their non-radiative relaxation occurs. Such process is a competing relaxation channel, comparing with the radiative relaxation (luminescence), and it should be very efficient in nanoparticles, where the role of surface states is dominated. Therefore, it is suggested that electrons and holes effectively trapped by the nanoparticle's surface and such surface-related loss processes are a main reason of luminescence vanishing under high energy excitations in nanosized $LaPO_4$:Ce,Tb. Negligible luminescence intensity of nanosized $LaPO_4$:Ce,Tb under high energy excitation definitely restricts these materials' utilization in some practical applications, for instance, as so-called "slow scintillators" for security applications.

The shape of the excitation spectra in the bulk $LaPO_4$ sample could depend on many different processes and parameters, which are considered in detail elsewhere. One of the most interesting processes occurring under high energy excitations is so-called multiplication of electronic excitations (MEE). MEE processes' creation means that two or more luminescence centers are created per one absorbed photon. For a successful realization of MEE processes, the excitation energy of the photon must exceed a threshold energy $E_{th} = 2E_g$, where E_g is the bandgap energy. MEE processes in wide bandgap materials were studied in detail in Refs. 62 and 63; however, such processes could be also successfully realized in semiconductor nanocrystals.[64,65] It is clearly seen from Fig. 4 that, for bulk $LaPO_4$:Ce,Tb, the rise of the excitation intensity for both Ce^{3+} and Tb^{3+} emissions starts at about 15-17 eV. This value is very close to the value of $2E_g$, keeping in mind that E_g in $LaPO_4$ is 8 eV.

B. YVO_4:Eu

Emission spectra for bulk and two nano (as-grown and YF_3-covered) YVO_4:Eu samples reveal the characteristic Eu^{3+} emission lines (Fig. 5), which are well known in the literature.[3,4,22,66] In contrast to the $LaPO_4$:Ce,Tb phosphor considered above in Subsection III A, the bandgap of YVO_4 is comparably small ($E_g \approx 3.4$ eV). It means that, even under comparably low 300-nm excitation, europium luminescence could be excited only after energy transfer from the YVO_4 matrix to Eu^{3+} ions with subsequent f-f radiative relaxation ($^5D_0 \rightarrow {}^7F_J$ transitions). Therefore, Eu^{3+} emission should be very sensitive to surface-related losses in YVO_4 nanoparticles. Surface-related losses mean that electronic excitations are captured by surface defects and/or imperfections with subsequent non-radiative annihilation. Under band-to-band excitation, electrons and holes form an excited intrinsic molecular complex $(VO_4)^{3-}$. The energy transfer from the $(VO_4)^{3-}$ complex to the activator ion leads to Eu^{3+} emission. However, electrons and holes could be also trapped on the surface instead of the formation of the $(VO_4)^{3-}$ complex. Therefore, surface-related loss could be considered as one of the competing relaxation channels under band-to-band excitation in nanoparticles.

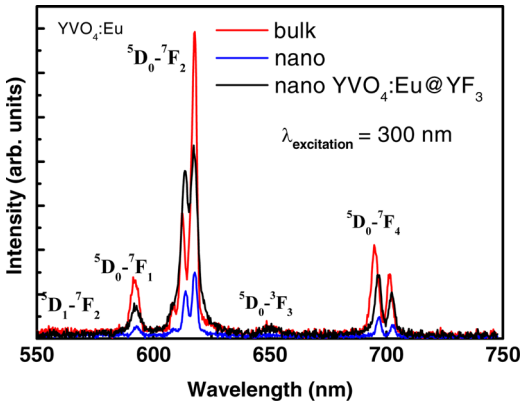

FIG. 5. (Color online) Emission spectra of Eu^{3+} ions in the macroscopic, nanosized, and nanosized YF_3-covered YVO_4:Eu at 10 K.

We did not compare quantum yields for three samples; however, special experiment conditions were provided for in order to compare intensities of luminescence for these three samples. It is clear (Fig. 5) that luminescence intensity drops down in the nanopowder, comparing with the bulk material. On the other hand, after surface passivation by the core shell layer, luminescence intensity could by significantly increased.

It is interesting to note that, in contrast to the emission spectra of $LaPO_4$:Ce,Tb depicted in Fig. 1, the fine structure of Eu^{3+} emission bands is well resolved even in YVO_4:Eu nanocrystals. It could mean that crystal field symmetry around Eu^{3+} ions does not suffer from the nanoparticle's surface.

The excitation spectra for Eu^{3+} emission in the three samples studied are depicted in Fig. 6–the low energy part is shown in detail in Fig. 6(a), whereas the whole spectra are demonstrated in Fig. 6(b). These spectra are normalized for better comparison. At least three peaks could be resolved in the excitation spectra for all samples studied: at 4 eV, 5 eV, and 6 eV (Fig. 6(a)). Similar peaks were observed before for bulk YVO_4:Eu in Ref. 67 (dashed line in Fig. 6(a)). Taking into account that similar excitation spectra are observed for YVO_4:Eu samples, which were produced by different methods, we can conclude that the structure of the excitation spectra in the 3.5–7.0 eV spectral range has intrinsic nature. For instance, we suppose that the density of states of vanadate bands is responsible for the structure of the excitation spectra.

The most significant distinction in the excitation spectra between bulk and nano YVO_4:Eu is observed in the high energy part (Fig. 6(b)). The excitation spectrum for bulk YVO_4:Eu has a strong rise at energies higher than 10 eV, reaching maximum at 30 eV. It is necessary to note that the intensity of the excitation peak at 30 eV is very close to the most intensive peak at 4 eV. Such strong intensive excitation

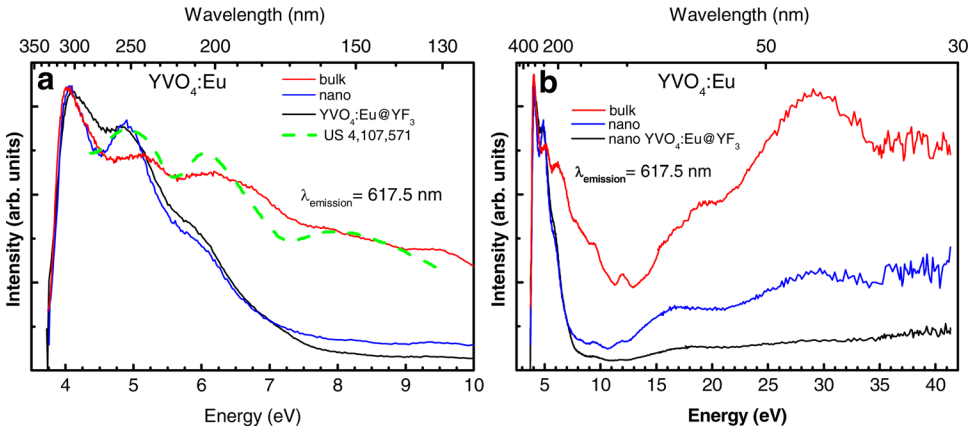

FIG. 6. (Color online) Excitation spectra of Eu^{3+} (617.5 nm) emission in the bulk, nanosized, and nanosized YF_3-covered YVO_4:Eu at 10 K in 3.5–10 eV (a) and 3.0–40 eV (b) spectral ranges. The excitation spectrum of Eu^{3+} taken from Ref. 67 (dashed line) is given in (a) for comparison.

of Eu^{3+} emission with photons with energies near 25 eV could have a practical application, for instance, in helium discharge lamps, taking into account the first ionization potential 24.581 eV of helium gas. Unfortunately, the origin of the intensive excitation in the 10–40 eV range in bulk YVO_4:Eu is unclear so far, and further investigation is required.

Exploring the excitation spectra for nanosized YVO_4:Eu and nanosized core shell-covered YVO_4:Eu, we can conclude that MEE processes are strongly suppressed there. Indeed, intensity of the excitation peak at 30 eV in nanosized YVO_4:Eu is about 30%, but in nanosized YVO_4:Eu@YF, it is about 10%, comparing with the bulk sample. The degradation of the excitation spectrum in nano YVO_4:Eu could be explained by an analogy with $LaPO_4$:Ce,Tb, considered above, i.e., by charge carriers trapping by surface defects with subsequent non-radiative relaxation. On the other hand, it is surprising that surface passivation by the nanoparticle covering in the YVO_4:Eu@YF sample does not increase the intensity of the excitation peak in the 10–45 eV range. Moreover, the intensity of this peak even decreases. It was expected that surface covering should passivate the surface defects, which are responsible for surface losses' processes, but in reality, we got the opposite result. It is necessary to note that the main difference between excitation spectra for nano YVO_4:Eu and YVO_4:Eu@YF_3 samples starts at energies higher than 10 eV (Fig. 6(b)) Taking into account that the bandgap energy of YF_3 is about 11 eV,[51] it is supposed that the YF_3 layer around the YVO_4:Eu nanoparticles works as a "shield", partially absorbing the excitation energy intended for the YVO_4:Eu core.

IV. CONCLUSION

Detailed investigation of luminescence properties of nano and macro-sized $LaPO_4$:Ce,Tb and YVO_4:Eu phosphors has been done in a wide spectral range, including the vacuum ultraviolet spectral range. It was demonstrated that nanoparticles' surface can drastically change emission and excitation spectra of nanopowders, comparing with corresponding bulk materials. Especially significant distinctions between excitation spectra for nano and bulk materials were observed under relatively high energy excitation (exceeding 10 eV). It was suggested that surface-related loss processes, namely electron-hole pairs' non-radiative annihilation at the surface, are responsible for the suppression of energy transfer processes from the host lattice to impurity ions and, subsequently, for rare-earth emission degradation under high energy excitations in nanosized materials.

ACKNOWLEDGMENTS

The experiments at DESY leading to these results have received funding from the European Community's Seventh Framework Programme (FP7/2007-2013) under grant agreement No. 226716. The work of V. Pankratov and L. Shirmane was granted by ESF Project No. 2009/0202/1DP/1.1.1.2.0/09/APIA/VIAA/141. The research of A.I. Popov was partially supported by Sadarbības projekts No. 10.0032.

[1]A. K. Levine and F.C. Palilla, Appl. Phys. Lett. **5**, 118 (1964).
[2]A. Bril, W. L. Wanmaker, and J. Broos, J. Chem. Phys. **43**, 311 (1965).
[3]K. Riwotzki and M. Haase, J. Phys. Chem. B **102**, 10129 (1998).
[4]K. Riwotzki and M. Haase, J. Phys. Chem. B **105**, 12709 (2001).
[5]T. Minami, T. Miyata, Y. Suzuki, and Y. Mochizuki, Thin Solid Films **65**, 469 (2004).
[6]A. Huignard, T. Gacoin, and J. Boilot, Chem. Mater. **12**, 1090 (2000).
[7]A. Huignard, V. Buissette, A. Franville, T. Gacoin, and J. Boilot, J. Phys. Chem. B **107**, 6754 (2003).
[8]M. Yu, J. Lin, Z. Wang, J. Fu, S. Wang, H. J. Zhang, and Y. C. Han, Chem. Mater. **14**, 2224 (2002).
[9]F. M. Nirwan, T. K. Gundu Rao, P. K. Gupta, and R. B. Pode, Phys. Status Solidi A **198**, 447 (2003).
[10]D. K. Williams, B. Bihari, and B. M. Tissue, J. Phys. Chem. B **102**, 916 (1998).
[11]H. Zhang, M. Lü, Z. L. Xiu, G. J. Zhou, S. F. Wang, Y. Y. Zhou, and S. M. Wang, Mater. Sci. Eng. B **130**, 151 (2006).
[12]Y. J. Sun, H. J. Liu, X. Wang, X. G. Kong, and H. Zhang, Chem. Mater. **18**, 2726 (2006).
[13]L. M. Chen, Y. N. Liu, and K. L. Huang, Mater. Res. Bull. **41**, 158 (2006).
[14]P. Ghosh, A. Kar, and A. Patra, J. Appl. Phys. **108**, 113506 (2010).
[15]L. R. Singh and R. S. Ningthoujam, J. Appl. Phys. **107**, 104304 (2010).
[16]S. Okamoto, R. Uchino, K. Kobayashi, and H. Yamamoto, J. Appl. Phys. **106**, 013522 (2009).
[17]K. S. Shim, H. K. Yang, Y. R. Jeong, B. K. Moon, B. C. Choi, J. H. Jeong, J. S. Bae, S. S. Yi, and J. H. Kim, Appl. Surf. Sci. **253**, 8146 (2007).
[18]C. Breacher, H. Samelson, A. Lempicki, R. Riley, and T. Peters, Phys. Rev. **155**, 178 (1967).
[19]E. D. Reed and H. W. Moos, Phys. Rev. B **8**, 980 (1973).
[20]E. D. Reed and H. W. Moos, Phys. Rev. B **8**, 988 (1973).
[21]A. Huignard, T. Gacoin, and J. P. Boillot, Chem. Mater. **12**, 1090 (2000).
[22]A. Zharkouskay, H. Lünsdorf, and C. Feldmann, J. Mater. Sci. **44**, 3936 (2009).

[23]N. Hashimoto, Y. Takada, K. Sato, and S. Ibuki, J. Lumin. 48-49, 893 (1991).
[24]T. Norby and N. Christiansen, Solid State Ionics **77**, 240 (1995).
[25]Y. Hikichi, T. Ota, K. Daimon, T. Hattori, and M. Mizuno, J. Am. Ceram. Soc. **81**, 2216 (1998).
[26]Y. Fang, A. Xu, R. Song, H. Zhang, L. You, J. C. Yu, and H. Liu, J. Am. Chem. Soc. **125**, 16025 (2003).
[27]C. Feldmann, T. Jüstel, C. R. Ronda, and P. J. Schmidt, Adv. Funct. Mater. **13**, 511 (2003).
[28]G. J. McCarthy, W. B. White, and D. E. Pfoertsch. Mater. Res. Bull. **13**, 1239 (1978).
[29]A. Meldrum, L. A. Boatner, and R. C. Ewing, Phys. Rev. B **56**, 13805 (1997).
[30]K. Riwotzki, H. Meyssamy, H. Schnablegger, A. Kornowski, and M. Haase, Angew. Chem., Int. Ed. **40**, 573 (2001).
[31]S. Heer, O. Lehmann, M. Haase, and H. U. Güdel, Angew. Chem., Int. Ed. **42**, 3179 (2003).
[32]K. Riwotzki, H. Meyssamy, A. Kornowski, and M. Haase, J. Phys. Chem. B **104**, 2824 (2000).
[33]C. W. Struck, Short luminescence delay time phosphors, U.S. patent 3,104,2246 (1963).
[34]G. Blasse and B. C. Grabmaier, Luminescent Materials (Springer-Verlag, Berlin, 1994).
[35]Phosphor Handbook, edited by W. M. Yen and S. Shionoya (CRC Press, Boca Raton, FL, 1999).
[36]B. Dubertret, P. Skourides, D. J. Norris, V. Noireaux, A. H. Brivanloue, and A. Libchaber, Science **298**, 1759 (2002).
[37]T. Pellegrino, S. Kuders, T. Liedl, A. M. Javier, L. Manna, and W. Parak, Small **1**, 48 (2005).
[38]C. R. Patra, R. Bhattacharya, S. Patra, S. Basu, P. Mukherjee, and D. Mokhopadhyay, J. Nanobiotechnol. **4**, 11 (2006).
[39]W. van Schaik, S. Lizzo, W. Smit, and G. Blasse, J. Electrochem. Soc. **140**, 216 (1993).
[40]J. M. P. J. Verstegen, J. L. Sommerdijk, and J. G. Verriet, J. Lumin. **6**, 425 (1973).
[41]J.-C. Bourcet and F. K. Fonf, J. Chem. Phys. **60**, 34 (1973).
[42]Ph. Meunier-Beillard, B. Moine, C. Dujardin, X. Cieren, C. Pedrini, D. Huguenin, and V. Archambault, Radiat. Eff. Defects Solids **149**, 25 (1999).
[43]V. Pankratov, A. I. Popov, S. A. Chernov, A. Zharkouskaya, and C. Feldmann, Phys. Status Solidi B **247**, 2252 (2010).
[44]D. S. McClure and C. Pedrini, Phys. Rev. B **32**, 8465 (1985).
[45]B. Moine, C. Pedrini, and V. Ghiordanescu, J. Phys.: Condens. Matter **6**, 4093 (1994).
[46]S. A. Chernov, L. Trinkler, and A. I. Popov, Radiat. Eff. Defects Solids **143**, 345 (1998).
[47]E. Nakazawa and F. Shiga, J. Lumin. **15**, 255 (1977).
[48]U. Sasum, M. Kloss, A. Rohmann, L. Schwarz, and D. Haberland, J. Lumin. **72-74**, 255 (1997).
[49]H. H. Rüter, H. V. Seggern, R. Reininger, and V. Saile, Phys. Rev. Lett. **65**, 2438 (1990).
[50]M. Kirm, G. Zimmerer, E. Feldbach, A. Lushchik, Ch. Lushchik, and F. Savikhin, Phys. Rev. B **60**, 502 (1999).
[51]V. Pankratov, M. Kirm, and H. von Seggern, J. Lumin. **113**, 143 (2005).
[52]V. Pankratov, L. Grigorjeva, S. Chernov, T. Chudoba, and W. Lojkowski, IEEE Trans. Nucl. Sci. **55**, 1509 (2008).
[53]A. Kalinko, A. Kotlov, A. Kuzmin, V. Pankratov, A. I. Popov, and L. Shirmane, Cent. Eur. J. Phys. **9**, 432 (2011).
[54]V. Pankratov, A. I. Popov, A. Kotlov, and C. Feldmann, Opt. Mater. **33**, 1102 (2011).
[55]G. Bühler and C. Feldmann, Angew. Chem., Int. Ed. **45**, 4864 (2006).
[56]G. Bühler and C. Feldmann, Appl. Phys. A **87**, 631 (2007).
[57]A. Zharkouskaya, C. Feldmann, K. Trampert, W. Heering, and U. Lemmer, Eur. J. Inorg. Chem. 873 (2008).
[58]G. Zimmerer, Radiat. Meas. **42**, 859 (2007).
[59]E. A. Kotomin and A. I. Popov, Nucl. Instrum. Methods Phys. Res. B **141**, 1 (1998).
[60]A. I. Popov, E. A. Kotomin, and J. Maier, Nucl. Instrum. Methods Phys. Res. B **268**, 3084 (2010).
[61]E. Nakazawa and F. Shiga, Jpn. J. Appl. Phys. **42**, 1642 (2003).
[62]M. Kirm, I. Martinson, A. Lushchik, K. Kalder, R. Kink, Ch. Lushchik, and A. Löhmus, Solid State Commun. **90**, 741 (1994).
[63]A. Lushchik, A. M. Kirm, Ch. Lushchik, I. Martinson, V. Nagirnyi, F. Savikhin, and E. Vasil'chenko, Nucl. Instrum. Methods Phys. Res. A **537**, 45 (2005).
[64]V. Pankratov, V. Osinniy, A. Kotlov, A. Nylandsted Larsen, and B. Bech Nielsen, Phys. Rev. B **83**, 045308 (2011).
[65]M. C. Beard, K. P. Knutsen, P. Yu, J. M. Luther, Q. Song, W. K. Metzger, R. J. Ellingson, and A. J. Nozik, Nano Lett. **7**, 2506 (2007).
[66]M. Haase, K. Riwotzki, H. Meyssamy, and A. Kornowski, J. Alloys Compd. **191**, 303 (2000).
[67]S. Tanimizu, T. Suzuki, and T. Fukuzawa, Light emitting device having luminescent screen with self activated blue light emitting phosphor, U.S. patent 4,107,571 (1978).